TELAC REPORT 95-11

COUPLED MATERIALS AND MECHANICS ANALYSES OF DURABILITY TESTS FOR HIGH TEMPERATURE POLYMER MATRIX COMPOSITES

presented at the
ASTM Second Symposium on High Temperature and Environmental Effects on Polymeric Composites
Norfolk, VA

Hugh L. McManus and Ronan A. Cunningham
Assistant Professor Research Assistant

November, 1995

Coupled Materials and Mechanics Analyses of Durability Tests for High Temperature Polymer Matrix Composites

Presented at the Second Symposium on High Temperature and Environmental Effects on Polymeric Composites, Norfolk, VA, on November 13, 1995

Hugh L. McManus and Ronan A. Cunningham

Class of 1943 Assistant Professor and Research Assistant
Technology Lab for Advanced Composites
Department of Aeronautics and Astronautics
Massachusetts Institute of Technology
77 Massachusetts Ave., Cambridge, MA 02139

A complete coupled model of the environmentally-induced degradation of composite materials, and the effect of this degradation on composite laminate behavior, is presented. Although the model is not sufficiently mature for predictive design use, it provides major insights into the mechanisms of degradation of composite materials. The model is used to study test methods frequently used to assess composite durability, including weight loss, shrinkage, and mechanical property degradation testing. It is found that even simple tests of material undergoing environmentally-induced degradation are difficult to interpret. In particular, the spatial non-uniformity of degradation converts originally simple specimens into complex structures with non-uniform chemical and mechanical states. Consideration of this complexity is vital to the full understanding of the results of such tests.

Composite materials are increasingly used in demanding structural applications, exposed to harsh environmental conditions. The durability of such materials is a major concern, potentially limiting both the integrity of the structures and their useful lifetime. High temperatures, thermal cycling, and exposure to moisture, oils, and solvents all accelerate the degradation of composites. Hence, application of composites to structures such as turbine engine components and high speed aircraft airframes may be ultimately limited by durability issues.

The present work is an attempt at developing an overall understanding of the mechanisms involved in composite degradation using a material modeling approach. A coupled model incorporating diffusion of oxygen into the material, degradation chemistry, matrix shrinkage and property loss, resulting effects on the ply and laminate level, and structural behavior of the degraded laminate is presented.

The model is used to replicate the results of a number of tests commonly used to study degradation effects in composite materials. Weight loss from rectangular prism specimens, the shrinkage and cracking of such specimens, cracking of laminates, and the degradation of measured properties from bending tests are all simulated as functions of time, temperature, and environmental conditions. The results are correlated with test results. They are also explored in detail using parametric studies to elucidate the mechanisms responsible for the behaviors observed.

Background

Extensive testing has been carried out to characterize the performance of polymer matrix composites at high temperatures. This paper will concentrate on a commonly used material system, the NASA-Lewis developed PMR polyimide material. Other materials, notably other polyimide thermosets, and thermoplastic materials such as PEEK, have also been included in aging studies. Many of the phenomena observed are similar to those reported for PMR materials. Recent development efforts in the PMR material system are discussed in [1]. Most testing has concentrated on isothermal aging, i.e. the effects of continuous soaking at a single high temperature [2-12].

Experimental studies of the effects of aging at elevated temperatures can be divided into two categories–aging in inert atmospheres and aging in air. They can also be divided by the nature of the material tested. Various investigations have considered neat resin [7,13], bare fibers [6] and composite materials [6,8,12,14,15]. Only limited correlation exists between individual studies.

Neat resin studies provide insight into major composite degradation mechanisms. The observed effects of long term aging on neat resin include specimen weight loss, specimen shrinkage, the formation of a distinct surface layer, development of surface microcracks and the degradation of mechanical properties. Weight loss appears to be the result of two mechanisms–thermal and oxidative. Thermal weight loss occurs within the first 100-200 hours of aging, is a bulk mechanism, i.e. depends only on specimen volume, and does not alter the physical nature of the polymer significantly, i.e. there is no evidence of an altered layer on the surface, voids or cracks [11].

Oxidative weight loss occurs throughout the aging periods observed. Over extended aging times a distinctive thin layer forms on the exposed surfaces and progresses inward. The surface layer exhibits a different chemical composition than the unreacted core material [7, 12]. Voids develop within the surface layer and increase in size and density over time. These voids act as starter points for microcracks which grow from the exposed surface. Similarity of observed surface layer growth rates and weight loss rates [7] suggests that the weight loss occurs primarily

in the degraded surface layer. Shrinkage of the polymer is also observed. It results in dimensional changes that are sensitive to specimen geometry.

Unidirectional composites demonstrate similar degradation mechanisms to the neat resin, although the weight loss is less severe. Weight loss appears to be dependent upon the matrix volume fraction [14]. Unidirectional composites also exhibit different rates of growth of surface degradation layers in each of the three principal directions–axial, transverse and through-thickness. Highly enhanced degradation occurs along the fiber-matrix interface, accelerating growth of surface layers in the axial direction. Growth of surface layers in the transverse and through-thickness directions is slower that in the axial direction [16], except when resin-rich molded surfaces are present [17]. In these cases, the growth rate is initially enhanced but as time progresses the growth rate returns to the rate seen on surfaces without extra resin.

General composites, which have plies at different angles, exhibit a more rapid weight loss than unidirectional composites. The weight loss at longer aging times in cross-plied composites appears to depend only on the specimen volume [18]. Again, a surface layer forms (approximately one ply thick) and microcracks develop at the surface. However, microcracks also form in the interior of the composite. Tensile stresses develop in the matrix due to residual thermal stresses from curing and degradation induced shrinkage, leading to cracking of the matrix throughout the laminate. The cracks in the laminate enhance oxidation of the composite by providing additional paths for air to penetrate the material. This can lead to a vicious circle, with oxidation promoting cracking, allowing more oxidation, and so on [18].

Attempts have been made to analyze and model various aspects of this problem. Mass loss rates have been empirically fitted to Arrhenius rate curves [9, 19]. This approach provides a simple means to model the stability of many different systems but is most useful as a comparative model if the physics of the mass loss are not separated out. More sophisticated models have combined modeling of the diffusion of oxygen into the material with chemical reaction rate equations to predict mass loss and the growth of degraded layers. In many such cases an effective diffusion coefficient model is used [8, 17]. In these cases an apparent diffusivity is found based on the experimental weight loss curve for a composite. Cracking of the degraded layers has been predicted by modeling the degraded layers as layers with different material properties in a finite element model [4]. Aging induced changes in viscoelastic properties have been incorporated into standard viscoelastic analysis techniques [5].

More general analysis techniques are also available that can be applied to some aspects of this problem. Here, only those used during this work are noted. Micromechanical models allow the prediction of composite properties and behavior given the matrix and fiber properties [20]. The effects of temperature and moisture on composite properties can also be predicted [21,22]. Existing semi-empirical analysis methods for composite durability [23] could be applied to this problem, although success is unlikely as these methods do not account for the unique physics observed in the high temperature degradation process.

Problem Statement

Given material properties (including chemical reaction constants, gas diffusivities and mechanical properties), geometry (including composite volume fractions and lay-up) and the environment (temperature and surface environment, as functions of time), predict the extent of oxygen diffusion into the material, the chemical state of the matrix, matrix shrinkage and property losses, and resulting ply and laminate properties and behavior.

Model

Approach

A model of the behavior of degrading composites is developed from basic engineering principles. Emphasis is placed on modeling all relevant phenomena and their possible interactions; therefore, the modeling of each phenomenon is kept as simple as possible. The model consists of the following submodels:

- Fickian model of diffusion of oxygen from the environment
- Arrhenius model of degradation chemistry
- Empirical matrix shrinkage and mechanical property loss model
- Micromechanical model of effects at the ply level
- Laminated plate model

The first two models will be presented and their coupled implementation discussed. The next three models, referred to here as the mechanical models, are fully described in [26]. The critical features of these models, and the coupling between the diffusion and chemistry models and the mechanical models, will be summarized here.

A flat plate of thickness $2h$ is considered. Its width and length are assumed to be much greater than its thickness. It is composed of unidirectional composite plies of thickness t, aligned to a reference axis at angle θ. Uniform in-plane loads **N** and moments **M** (stress resultants in the notation of Jones, [24]) are applied at the edges. One or both faces are exposed to an oxygen-containing atmosphere at time-varying temperature T and pressure P. It as assumed that the thermal transient time is small compared to that of all degradation mechanisms, so the temperature throughout the plate is assumed to be T.

Diffusion Model

It is assumed that substances from the environment diffuse into the material according to the following modified Fickian diffusion law.

$$\frac{\partial c_s}{\partial t} = \frac{\partial}{\partial x_i}\left(D_{ij}^s \frac{\partial c_s}{\partial x_j} \right) - r_s \tag{1}$$

where c_s is the relative concentration of substance s, D_{ij}^s is the non-isotropic tensor of diffusivity of substance s through the composite material, and r_s is the rate of consumption of substance s by reactions. The calculation of r_s is discussed below. The relative concentration c_s is defined such that when $c_s = 1$ the material is locally saturated with substance s, while $c_s = 0$ indicates its absence. The diffusivity constants D_{ij}^s are strongly dependent on temperature. Typically [25]

$$D_{ij}^s = D_o e^{-C/T} \tag{2}$$

where D_o and C are constants. Generally, a different D_o and C are possible for each component of D_{ij} and for each substance s.

Degradation Chemistry Model

Simple Arrhenius reactions are assumed. The reactions may be temperature dependent only (representing thermal breakdown of material) in which case the reaction rates as described by

$$\frac{\partial \alpha_r}{\partial t} = k_r (1-\alpha_r)^{p_r} \exp\left(\frac{-E_r}{RT}\right) \tag{3}$$

where α_r is a measure of the completeness of reaction r, and k_r , p_r and E_r are the rate constant, order, and activation energy of the reaction respectively. The metric α_r is taken to be equal to zero at the beginning of the reaction, and one at the end.

Oxidative reactions (or, more generally, reactions requiring any substance k diffusing from the environment) are modeled using the following rate law, where q_r is the order of the concentration dependence.

$$\frac{\partial \alpha_r}{\partial t} = k_r (1-\alpha_r)^{p_r} c_s^{q_r} \exp\left(\frac{-E_r}{RT}\right) \tag{4}$$

Implementation of Coupled Diffusion/Chemical Model

The diffusion and chemistry models are implemented using a 1-D computer code. Oxygen concentration and degradation due to a single oxidative reaction are predicted as functions of time and distance z from the surface. These quantities are assumed to vary continuously through the thickness, so a large number of computational nodes are used. From Eq. 1,

$$\frac{\partial c_{ox}}{\partial t} = D_{zz}^{ox} \frac{\partial^2 c_{ox}}{\partial z^2} - r_{ox} \tag{5}$$

and from Eq. 4

$$\frac{\partial \alpha_{ox}}{\partial t} = k_{ox} (1-\alpha_{ox})^{p_{ox}} c_{ox}^{q_{ox}} \exp\left(\frac{-E_{ox}}{RT}\right) \tag{6}$$

The consumption rate of oxygen r_{ox} is found from the reaction rate

$$r_{ox} = R_{ox} \frac{\partial \alpha_{ox}}{\partial t} \tag{7}$$

where R_{ox} is a constant dependent on the chemistry of the reaction. The reduction in solid mass due to reactions is also dependent on the chemistry of the reactions. It can be expressed as

$$m = m_o - m_r \alpha_{ox} \tag{8}$$

Here, m, m_o and m_r represent the mass per unit *original* volume, the original mass per unit volume, and the change in mass per unit original volume when the reaction is complete. Note m is not necessarily equal to the material density, as the material may shrink during degradation, changing the volume. If the material does not shrink, m equals the local material density ρ. The total mass lost from a specimen of width W, length L, and thickness $2h$ is then

$$\Delta M = 2WL \int_0^h (m_o - m)\, dz \tag{9}$$

Equations 5-9 are solved numerically using an explicit finite difference scheme to predict oxygen concentrations, reaction rates, reaction states, and mass loss as functions of time and position, and total mass loss as a function of time. Initial conditions are $c_{ox} = 0$ and $\alpha_{ox} = 0$ everywhere. Boundary conditions are $c_{ox} = 1$ at the surface ($z = 0$), and no mass flux ($\partial c_{ox}/\partial z = 0$) at the midplane of the plate ($z = 0$)

Matrix Shrinkage and Mechanical Property Loss Model

The mechanical modeling of the degradation effects is performed on a ply-by-ply basis. Thus, the progress of the oxidation reaction α_{ox}, which is a continuous function of z, is averaged across each ply. The result is the matrix degradation metric b. Taking the definition of b found in [26] and averaging across a given ply k

$$b_k = \frac{1}{t_k}\int_{z_k^b}^{z_k^t} \frac{m_o - m}{m_o}\, dz \tag{10}$$

Where t_k is the ply thickness, and z_k^t and z_k^b are the positions of the top and bottom of ply k, respectively. Substituting Eq. 8 into Eq. 10 yields

$$b_k = \frac{m_r}{t_k\, m_o}\int_{z_k^b}^{z_k^t} \alpha_{ox}\, dz \tag{11}$$

showing that b_k is simply an expression of the average chemical degradation in the ply.

Matrix properties are assumed to degrade as a (empirical) function of b_k. Matrix degradation also causes an increase in void content ϕ found from

$$\phi = \phi_o + Db \tag{12}$$

where ϕ_o is the initial void content and D is an experimentally determined constant. Mass loss not arising from the formation of voids is assumed to cause shrinkage, hence

$$\varepsilon_b^* = -\frac{(1-D)b}{3} \tag{13}$$

The shrinkage strain resembles a thermal strain. In a uniformly shrinking body free of restraint it will not induce stress, but in a non-uniformly shrinking body and/or one in which deformations are restrained, it can induce stresses.

Ply Level Model

The property changes in, and shrinkage of, the matrix causes property changes in, and shrinkage of, unidirectional composite plies. The effects are calculated for each ply k in the laminate. The ply properties are calculated by assuming that the fiber properties do not degrade and the fibers do not shrink. Micromechanical techniques are used to determine the changes in ply properties due to changes in the matrix properties [26].

The shrinkage of the matrix also causes shrinkage of the plies. A modified set of micromechanical relations are used to calculate ply deformations due to matrix shrinkage . These

relations, combined with Eq. 13, yield relations between ply shrinkage and the degradation metric b of the form

$$\varepsilon_{11}^{*} = \chi_{11} b \qquad \varepsilon_{22}^{*} = \chi_{22} b \tag{14}$$

where ε_{11}^{*} and ε_{22}^{*} are ply shrinkage strains in the longitudinal and transverse directions, and the χ's are shrinkage strain coefficients, derived in [26].

The in-plane stress-strain behavior of the degraded ply can now be described by

$$\boldsymbol{\sigma} = \mathbf{Q}\left(\boldsymbol{\varepsilon} - \boldsymbol{\varepsilon}^{T} - \boldsymbol{\varepsilon}^{H} - \boldsymbol{\varepsilon}^{*}\right) \tag{15}$$

or equivalently

$$\boldsymbol{\sigma} = \mathbf{Q}\left(\boldsymbol{\varepsilon} - \boldsymbol{\alpha}\Delta T - \boldsymbol{\beta}\Delta M - \boldsymbol{\chi} b\right) \tag{16}$$

where $\boldsymbol{\sigma}$ is the ply in-plane stress vector, and $\boldsymbol{\varepsilon}$, $\boldsymbol{\varepsilon}^{T}$, $\boldsymbol{\varepsilon}^{H}$, and $\boldsymbol{\varepsilon}^{*}$ are the corresponding vectors of strain, thermal strain, hygral strain, and shrinkage strain, and $\boldsymbol{\alpha}$, $\boldsymbol{\beta}$, and $\boldsymbol{\chi}$ are the thermal, hygral, and shrinkage coefficient vectors. The matrix $\mathbf{Q}$ is the reduced stiffness matrix, calculated using the degraded ply material properties.

Laminated Plate Model

Equation 16 can be used in place of the conventional stress-strain relations to derive a modified classical laminate plate theory to predict the stresses and strains in, and deformations of, a laminated plate. Ply property degradations affect laminate properties, and ply shrinkage can cause deformations of, and stresses in, the laminate. Failure criteria can be applied to determine which plies fail, and in what mode. Details are given in [26].

Implementation of Mechanical Models

The matrix degradation, ply, and laminate models are implemented as modules of the ICAN computer code. A complete description of this code is given in [20]; the new modules are described in [26]. The user specifies laminate geometry, loadings, temperatures, moisture contents, and degradation states. The user can also modify a material data base file containing constituent material properties and the constants relating degradation to material property changes. The output is a complete description of the laminate, including laminate properties and stresses and strains in all plies.

Results

In this section, results from three studies are presented. Mass loss from a finite size specimen is considered first. A fit to existing data is used to find approximate material constants, then a parametric study is used to explore the relative importance of diffusion and reaction rates to the degradations. The second study considers the shrinkage of a neat resin specimen of the type used in the mass loss studies. Finally, the effect of non-uniform degradation on the results of mechanical tests are considered.

Mass Loss Tests

As reported by Bowles, Jayne and Leonhardt [7], 75 mm × 6.4 mm samples of neat resin, either 6.4 mm or 2.5 mm thick, were isothermally exposed, and weight loss, shrinkage, and the depth of a visible surface layer measured. The tests are analytically simulated using the coupled diffusion and chemical reaction models. The constants needed to use the model were estimated from available literature. Bowles [6] reported the activation energy for the mass loss degradation mechanism to be 128 kJ/mol. Other studies have been carried out using thermogravimetric analyses to measure both activation energies and pre-exponential constants. Kiefer, Yue and Hinkley [19] performed tests on thermoplastic polyimides. The powdered samples used in these tests gave approximately the same activation energy (121 kJ/mol) as in [7]. For this reason it was decided to used the pre-exponential rate constant from this data as a starting point for determining the actual constants. Limited information on the gas diffusivity of polymer matrix composites was given in [8]. Water diffusivity is more widely studied. Values of D_o and C, which fall in a relatively narrow range, were reported in [25]. These were used as a starting point for further calculations.

Preliminary values in Table 1 were taken as a starting point, and then a fit to existing mass loss data [7] was used to establish constants. The fit achieved is shown in Figure 1. The resulting fit constants are also given in Table 1. These constants should not be considered useful for predictive calculations. Instead, they were used as a baseline for parametric calculations. No information on the quantities of oxygen absorbed into polymer surfaces was available, so the concentration c_{ox} was left as a relative, dimensionless parameter. No information was available on the consumption rate R_{ox}, so it was set to a nominal value of 0.01. The initial density m_o was set to 1 300 kg/m^3, and the mass loss per unit volume during the reaction m_r was taken to be 234 kg/m^3, based on the data from [7].

To compare the relative importance of the diffusion and reaction mechanisms, a non-dimensional parameter ζ is defined as

$$\zeta = \frac{k_{ox} h^2 e^{-E_{ox}/RT}}{D_{zz}^{ox}} \tag{17}$$

Large values of ζ indicate that the mass loss will be limited by diffusion; small values indicate that the reaction speed will limit the mass loss. If the consumption of the diffusing substance (r_k in Eq. 5) is not too large, ζ can be shown to fully characterize the shape of the mass loss curve.

A parametric study was carried out. Mass loss calculations were repeated for each set of D_{zz}^{ox} and k_{ox} values given in Table 2. These values were normalized such that the total mass loss at 1 000 hours was held constant at 37 mg in each set of calculations. The results are shown in Figures 2 and 3. Figure 2 shows that the shape of the mass loss vs. time curve depends on the parameter ζ. The effect of ζ can be seen even more clearly in Figure 3, which shows the mass loss rate. This figure includes the data of Bowles. It appears to confirm that in the case studied by Bowles, the reaction is limited by diffusion. It was found that for small values of r_{ox}, ζ entirely controls the shape of this curve. The value of ζ may be kept the same by simply increasing or decreasing both D and k in the same proportion. The effect this has is to speed up or slow down the overall reaction, but it does not change the curve shape.

The internal distributions of absorbed oxygen c_{ox} and oxidation reaction progress α are shown in Figures 4 and 5 for the case of $\zeta = 24\ 090$, the value which matched the mass loss data

of Bowles. It is seen that degradation proceeds in from the surface, paced by the availability of oxygen.

Figure 6 and 7 show the absorbed oxygen concentration and reaction progress in the case where $\zeta = 0.1$. Although not entirely uniform, degradation proceeds throughout the sample. By studying a complete set of such figures, it was determined that for ζ values below 1 000, the degradation process was reaction rate limited; for values from 1 000 to 5 000 it was dependent on both reaction rate and oxygen diffusion, and at values above 5 000 it was limited by the availability of diffused oxygen.

Bowles also recorded the progression of the observed degraded layer. Figure 8 compares Bowles' fit to his empirical data and the predictions of the model. It was assumed that when α=0.25 at a point in the specimen the degradation is visible at that point. The good agreement increases confidence that the model is capturing the correct phenomenon.

To parametrically study the effects of different temperatures, the dimensionless parameter ζ is reconsidered. To consider the temperature dependence of D_{zz}^{ox}, Eq. 2 is substituted into Eq. 17, which yields

$$\zeta = \frac{k_{ox} h^2}{D_o} e^{-(E_{ox}/R - C)/T} \tag{18}$$

A parametric study was carried out starting with the nominal values from the last line in Table 2, and varying temperature. The cases studied are summarized in Table 3. At different temperatures, the reactions proceed at very different rates. To allow a comparison of the different cases, the time scale was normalized by t_o, defined as the time necessary to reach 37 mg mass loss in each case. The value of t_o for each case is shown in Table 3. The resulting consolidated plot is shown in Figure 9. The waviness of the curve at T=300K is a numerical artifact, due to the extremely long times required (see Table 3). The mass loss curve shapes are very dependent on temperature. As noted before, the mass loss curve shape is determined by ζ, which also indicates the relative importance of diffusion and reaction rate mechanism. Table 3 shows a wide range of ζ values. Over practical ranges of testing and use, ζ appears to be very high, indicating diffusion dominated behavior. At higher (accelerated testing) temperatures, ζ is reduced but is still high enough to indicate that the degradation mechanism remains diffusion dominated.

Shrinkage

The specimens of Bowles were modeled using the ply and laminate behavior models to predict their shrinkage along their long axes. They were modeled as 3 layer laminates- two degraded layers and a central core that is not degraded. The thicknesses of the degraded layers were modified to account for the finite width of the specimens. This model is accurate for axial stress and shrinkage predictions, which depend solely on the relative areas of the degraded and undegraded material. Because of the changing degradation layer thickness, a new model was constructed for each temperature and exposure time.

The diffusion/chemical reaction model was used to define the degradation state of the specimen. The degraded layer thickness as a function of time was taken from predictions shown in Figure 8. The ply degradation metric b for the degraded plies was then calculated using Eq. 11. The ply model was used to find the response of the degraded layers, and the laminate model to find the shrinkage of the entire specimen.

The shrinkage of the specimen was predicted assuming no mechanical loads or residual thermal stresses. It was assumed that $D = 0.1$, based on the observation of moderate void formation in the degraded layer. The results are compared to the measured results in Figure 10. As can be seen, the correlation is quite good. The results are essentially identical to the results shown in [26]. In that case, the matrix degradation state was determined empirically, directly from Bowles' weight loss and degradation layer thickness data.

The results provide insight into the mechanisms of specimen shrinkage. The mass loss in the surface layer results in shrinkage, which is constrained by the unshrinking, undegraded core material. The result is a net shrinkage of the entire specimen, and stresses in both the degraded layers and the core. The core stress are compressive, and the stresses in the degraded layer are tensile. These stresses reach sufficient magnitude to cause failure in the degraded layer. Although insufficient data was provided in [7] for a quantitative correlation of this effect, the failure in the surface layers predicted by the code qualitatively agrees with the observed surface layer cracking.

Bend Test for Mechanical Properties

Three- or four-point bending tests are a simple way to extract material properties at high temperatures, but the results must be carefully interpreted. A 16-ply unidirectional laminate tested in [2] is analyzed. The coupled models were used to predict degradation in the surface plies after 150 hours at 371°C, the ply response to this degradation, and the laminate response to degradation and bending loads. This study is more fully described in [26]. The axial stress distribution in the laminate for the bending load just sufficient to fail the laminate is shown in Figure 11, along with the stresses predicted for a uniform material under the same load. The apparent step-wise variation in the stresses is an artifact of the code's calculation of a single stress for each ply, and is not important. However, the top and bottom plies have stresses that differ significantly from those predicted for a uniform material due both to shrinkage and changes in stiffness. These plies also have differing strengths than the core plies due to degradation. These effects complicate accurate interpretation of bending test data.

Conclusions

The models developed can replicate the observed physics of degrading polymer matrix composite materials. Mass loss, shrinkage property changes, cracking and failure, and their dependencies on temperature, time, and specimen geometry can be predicted with a coupled set of simple models.

The coupled diffusion and chemical reaction models provide insight into the mechanisms of degradation. A dimensionless parameter can be used to assess the relative importance of diffusion and chemical reaction rates in controlling the behavior of a degrading specimen. This parameter is dependent on material properties, specimen geometry, and test (or use) temperature. The behavior of neat PMR-15 resin specimens under accelerated test conditions seems to be governed by diffusion, and appears to become increasingly dominated by diffusion at lower (use) temperatures.

The predictions of the diffusion and chemical models can be used as input to models of degrading and shrinking ply and laminate behavior. These models can be used to predict the behavior of mechanical tests specimens. It is found that even simple tests such as neat resin sample shrinkage measurements are in fact measurements of complex behavior. Severely degraded surface layers shrink causing a lesser degree of overall specimen shrinkage, and setting up internal stresses which ultimately cause the surface layers to crack. Mechanically loaded specimens such as bending test specimens will behave in even more complex ways, with the mechanical loads,

material changes, and shrinkage-induced deformations and internal stresses all interacting. This complex behavior must be taken into account when interpreting the results of such tests.

It appears that relatively simple models of the relevant physical phenomenon can be combined to successfully predict the complex observed behavior of degrading composite laminates. These models provide insights into the mechanisms of degradation. They are also necessary tools for interpreting test results and designing accelerated tests. The usefulness of the models would be improved by both more sophisticated models and better material property data bases. In particular, the reaction chemistry and diffusion models currently use properties collected from several sources and then fit to existing data. The resulting data base provides useful insights but can not be used for predictive calculations.

Acknowledgments

This work was supported by National Science Foundation Young Investigator Award MSS-9257612 and NASA Lewis Grant NAG3-1760, under the direction of Dr. Christos C. Chamis.

References

1. Meador, M. A., Cavano, P. J., and Malaric, D. C., "High Temperature Polymer Matrix Composites for Extreme Environments", Proceedings of the Sixth Annual ASM/ESD Advanced Composites Conference, Detroit, MI, Oct. 1990, pp. 529-539.
2. Vannucci, R. D., and Cifani, D., "700°F Properties of Autoclave Cured PMR-II Composites", Proceedings of the 20th International SAMPE Conference, Sept. 1988, pp. 562-575.
3. Pederson, C. L., Gillespie, J. W. Jr., McCullogh, R. L., Rothschilds, R. J., and Stanek, S. L., "The Effect of Isothermal Aging on Transverse Crack Development in Carbon Fiber Reinforced Cross-Ply Laminates", CCM Report 93-42, University of Delaware Center for Composite Materials, Newark, DE, November 1993.
4. Pederson, C. L., "The Effect of Temperature on Transverse Cracking in High Performance Composites", CCM Report 92-28, University of Delaware Center for Composite Materials, Newark, DE, June 1992.
5. Gates, T. S, and Brinson, L. C., "Acceleration of Aging in Graphite/Bismaleimide and Graphite/Thermoplastic Composites", Proceedings of the 36th AIAA/ASME/ASCE/ AHS/ASC Structures, Structural Dynamics, and Materials Conference, Hilton Head, SC, April 1994, pp. 2096-2105.
6. Bowles, K. J., "Thermo-Oxidative Stability Studies of PMR-15 Polymer Matrix Composites Reinforced with Various Continuous Fibers", *SAMPE Quarterly,* Vol. 21, No. 4, 1990, pp. 6-13.
7. Bowles, K. J., Jayne, D., and Leonhardt, T. A., "Isothermal Aging Effects on PMR-15 Resin", *SAMPE Quarterly,* Vol. 24, No. 2, 1993, pp. 3-9.
8. Hipp, R. C., Harmon, D. M., and McClellan, P. S., "Accelerated Aging and Methodology Development for Polymeric Composite Material Systems", McDonnell Douglas Co. preprint, 1994.
9. Grayson, M. A., and Fry, C. G., "On the Use of a Kinetic Map to Compare the Thermal Stability of Polymeric Materials Undergoing Weight Loss", McDonnell Douglas Co. preprint, 1994.

10. Bowles, K. J., and Nowak, G., "Thermo-Oxidative Stability Studies of Celion 6000/PMR-15 Unidirectional Composites, PMR-15, and Celion 6000 Fiber", *Journal of Composite Materials,* Vol. 22, 1988, 966-985.

11. Bowles, K. J., "A Thermally Modified Polymer Matrix Composite Material with Structural Integrity to 371°C", Proceedings of the 20th International SAMPE Conference, Sept. 1988, pp. 552-561, also published as NASA TM-100922.

12. Martin, R. H., Siochi, E. J., and Gates, T. S., "Isothermal Aging of IM7/8320 and IM7/5260", Proceedings of the American Society for Composites 7th Technical Conference on Composite Materials, University Park, PA, Oct. 1992, pp. 207-217.

13. Alston, W.B., Gluyas, R.E. and Snyder, W.J., "Cyclopentadiene Evolution During Pyrolysis-Gas Chromatography of PMR Polyimides", Proceedings of the Fourth International Conference on Polyimides, Ellenville, NY, October 30-November 1, 1991.

14. Alston, W.B., "Resin/Fiber Thermo-Oxidative Interactions in PMR Polyimide/Graphite Composites", Proceedings of Twenty-Fourth National SAMPE Symposium, San Francisco, CA, May, 1979.

15. Alston, W.B., "Characterization of PMR-15 Polyimide Resin Composition in Thermo-Oxidatively Exposed Graphite Fiber Composites", Proceedings of the Twelfth National SAMPE Technical Conference, Seattle, WA, October, 1980.

16. Madhukar, M.S., Bowles, K.J. and Papadopolous, D.S., "Thermo-Oxidative Stability of Graphite/PMR-15 Composites: Effect of Fiber Surface Modification on Composite Shear Properties", NASA TM-4608.

17. Nam, J.D. and Seferis, J.C., "Anisotropic Thermo-Oxidative Stability of Carbon Fiber Reinforced Polymeric Composites", *Sampe Quarterly*, Vol. 24, No. 1, October 1992, pp. 10-18.

18. Bowles, K.J., Jayne, D., Leonhardt, T.A., and Bors, D., "Thermal Stability Relationships Between PMR-15 Resin and Its Composites", *Journal of Advanced Materials*, Vol. 26, No. 1, October 1994, pp. 23-32.

19. Kiefer, R., Yue, J.J., and Hinkley, J.A., "Kinetic Mapping of Oxidative Weight Loss in Polyimide Composites", *Journal of Advanced Materials*, Vol. 26, No. 3, April 1995, pp. 55-59.

20. Murthy, P. L. N., Ginty, C. A., and Sanfeliz, J. G., "Second Generation Integrated Composite Analyzer (ICAN) Computer Code", NASA TP-3290, Jan. 1993.

21. Chamis, C. C., "Simplified Composite Micromechanics Equations for Hygral, Thermal, and Mechanical Properties", *SAMPE Quarterly*, Vol. 15, April 1984, pp. 14-23.

22. Chamis, C. C., "Simplified Composite Micromechanics for Predicting Microstresses", NASA TM-87295.

23. Chamis, C. C., and Ginty, C. A., "Fiber Composite Structural Durability and Damage Tolerance: Simplified Predictive Methods", NASA TM-1000179, April 1987.

24. Jones, R. M., *Mechanics of Composite Materials*, Hemisphere, New York, 1975.

25. Tsai, S.W., *Composites Design*, 4th. Edition, Think Composites, Ohio, 1988.

26. McManus, H.L., and Chamis, C.C., "Stress and Damage in Polymer Matrix Composite Materials Due to Material Degradation at High Temperatures", to be published as a NASA TM, 1995.

TABLE 1--Empirical/model chemical reaction data

	E_{ox}	E_{ox}/R(K)	log k_{ox}(s^{-1})	D_o(mm^2/s^{-1})	$C(K)$
Starting Point Data	128	15 395	7.81	16.1	5 690
Model Fit	128	15 395	6.81	4.31×10^4	18 000

TABLE 2--Parametric study values

ζ	log k_{ox}(s^{-1})	log D_{∞}^{ox} mm^2/s^{-1})
0.1	4.48	-6.27
10	5.13	-7.59
100	5.51	-8.21
1 000	5.95	-8.76
10 000	6.54	-9.18
20 000	6.74	-9.27
24 090	6.81	-9.30

TABLE 3--ζ and normalisation factor t_0 as functions of temperature

$T(K)$	ζ	t_o(hrs)
300	1.37×10^6	5.65×10^{14}
400	15 615	2.45×10^8
500	39 155	4.17×10^4
561	24 090	1.00×10^3
600	17 814	1.35×10^2
700	9 580	2.30

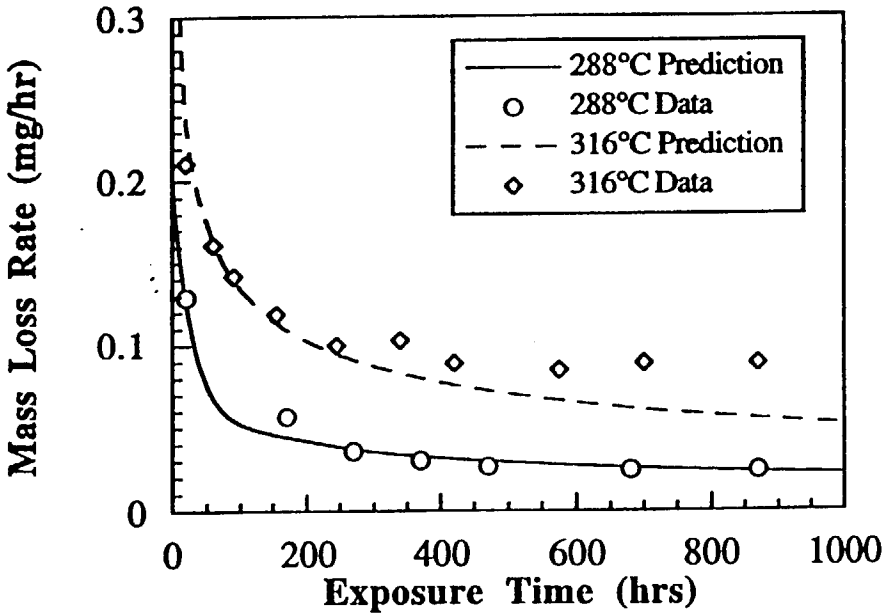

Figure 1. Comparison of predicted mass loss rate to data of Bowles at 288°C and 316°C.

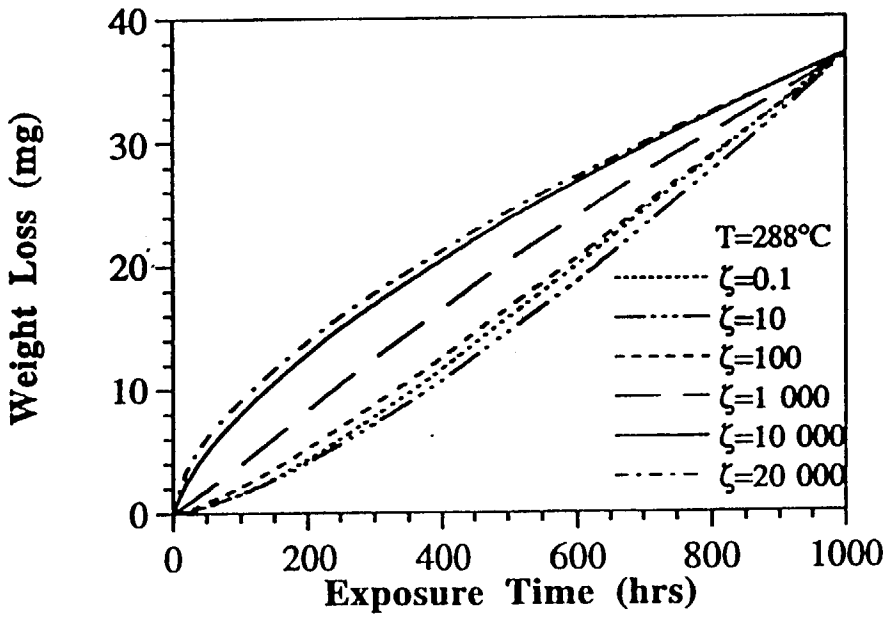

Figure 2. Mass loss as a function of time for different values of the dimensionless parameter ζ at 288°C.

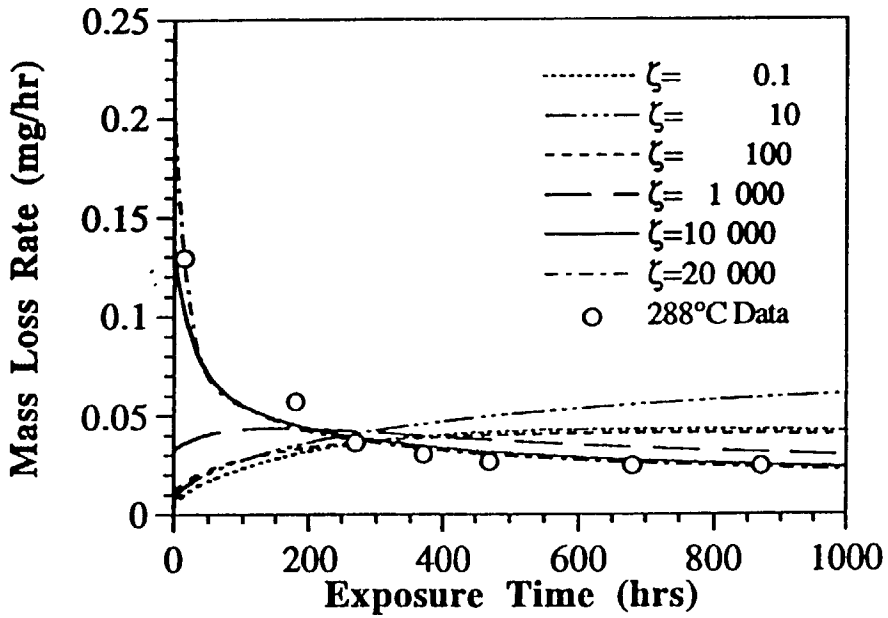

Figure 3. Mass loss rate as a function of time for different values of the dimensionless parameter ζ.

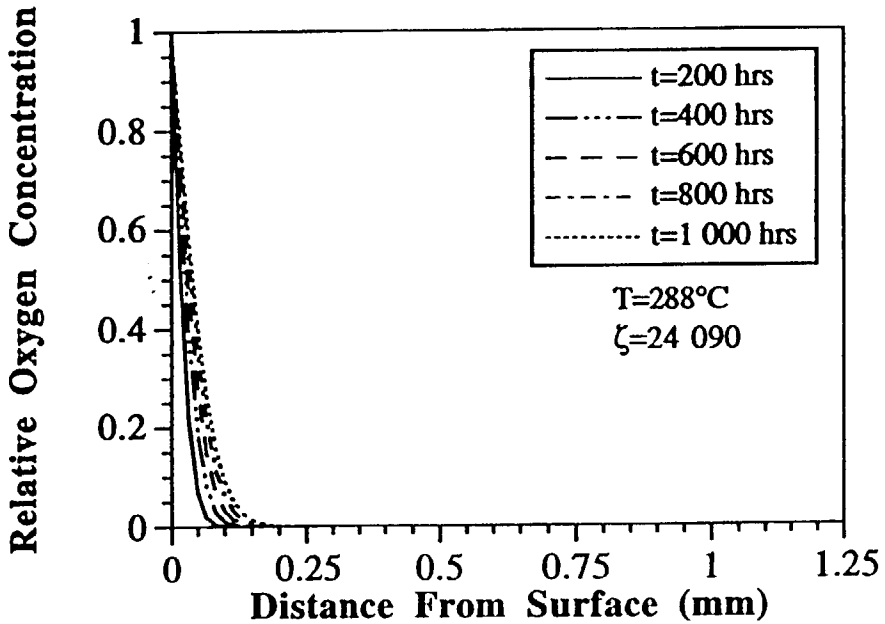

Figure 4. Relative oxygen concentration through specimen thickness at different times at 288°C for ζ=24 090.

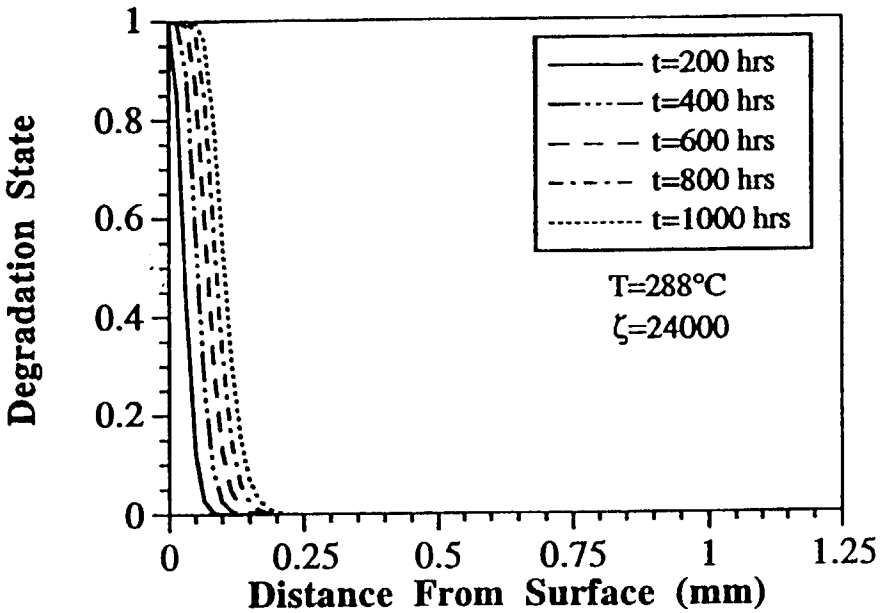

Figure 5. Degradation state through specimen thickness at different times at 288°C for ζ=24 090.

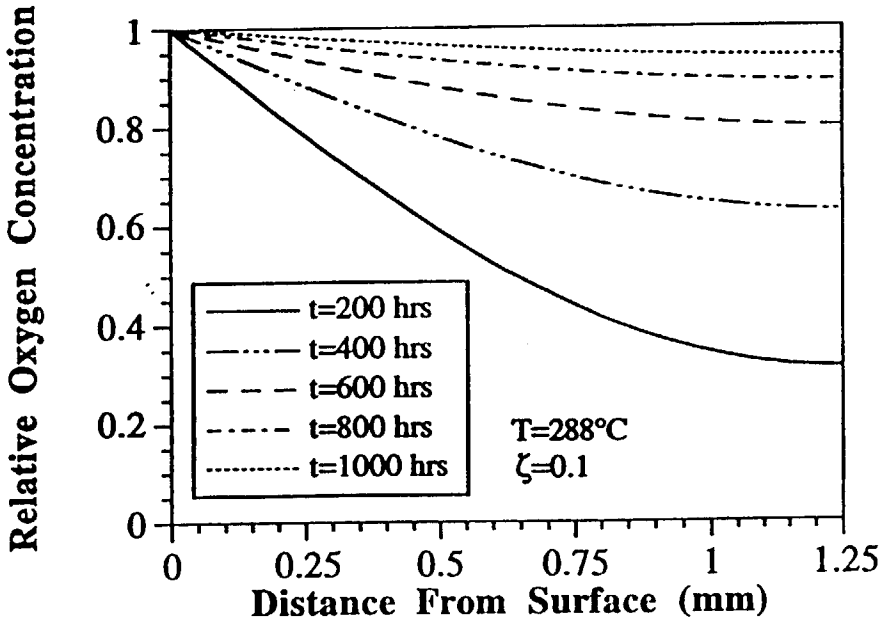

Figure 6. Relative oxygen concentration through specimen thickness at different times at 288°C for ζ=0.1.

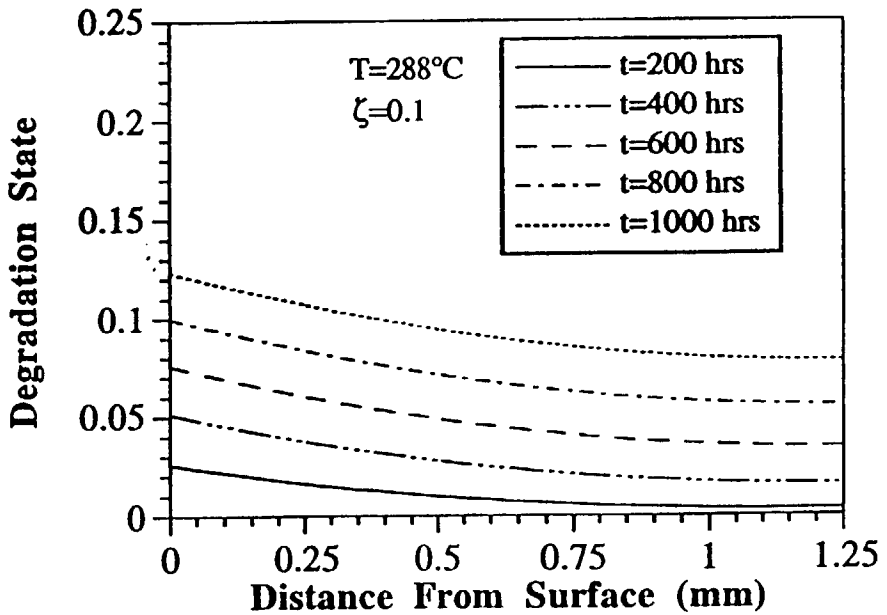

Figure 7. Degradation state through specimen thickness at different times at 288°C for ζ=0.1.

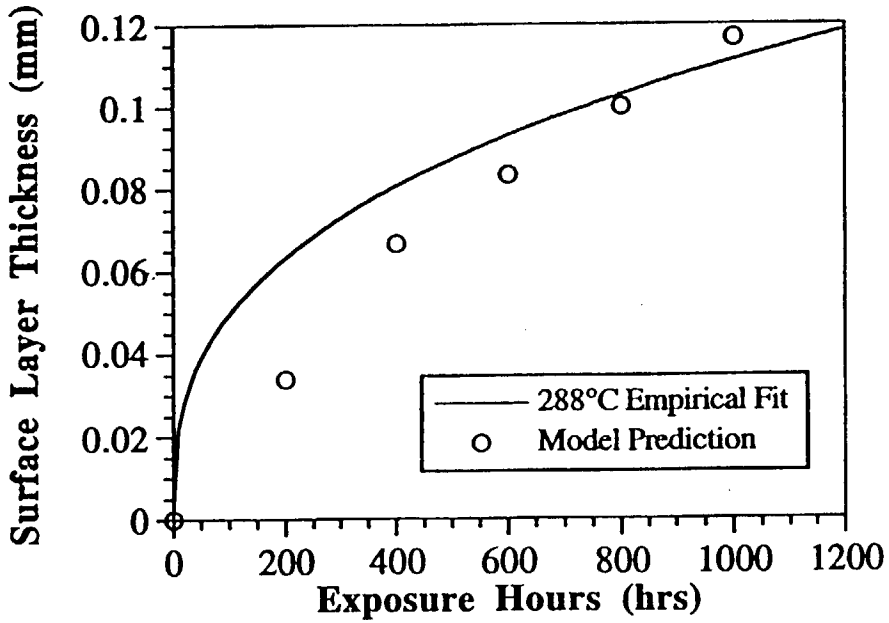

Figure 8. Comparison of predicted surface layer thickness to empirical data fit of Bowles at 288°C for ζ=24 090.

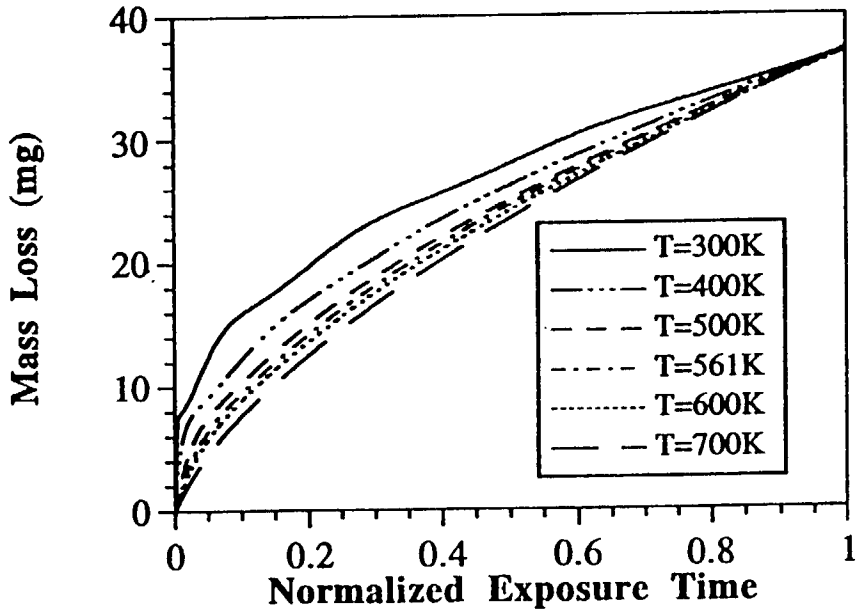

Figure 9. Comparison of mass loss curves at different temperatures for fixed set of reaction and diffusion constants.

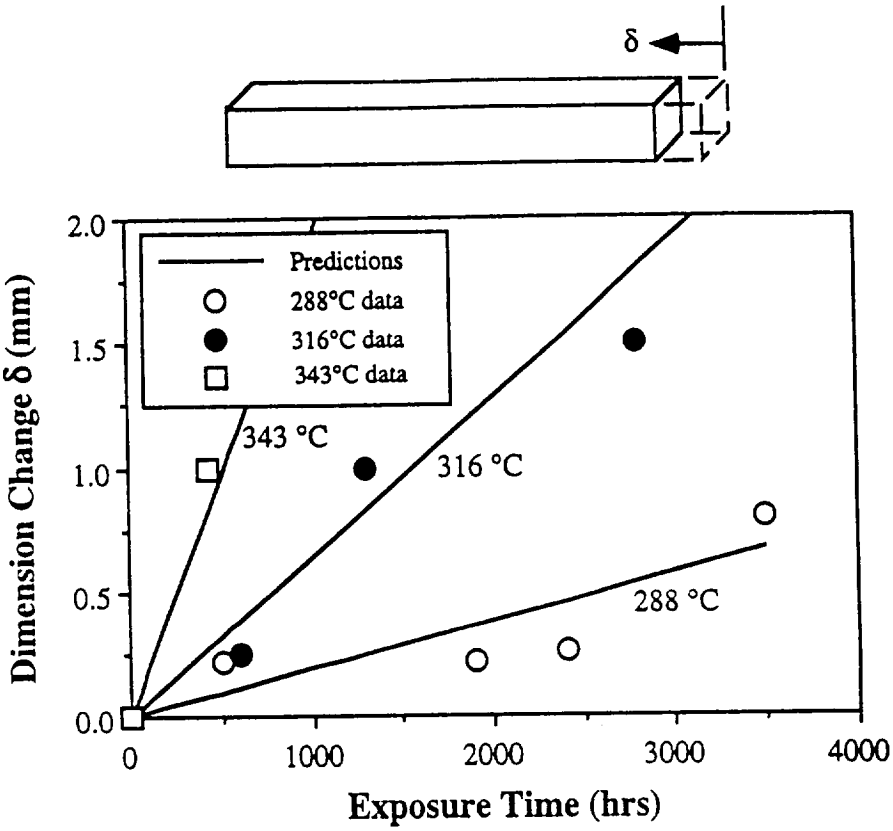

Figure 10. Comparison of predicted longitudinal dimension changes to data of Bowles.

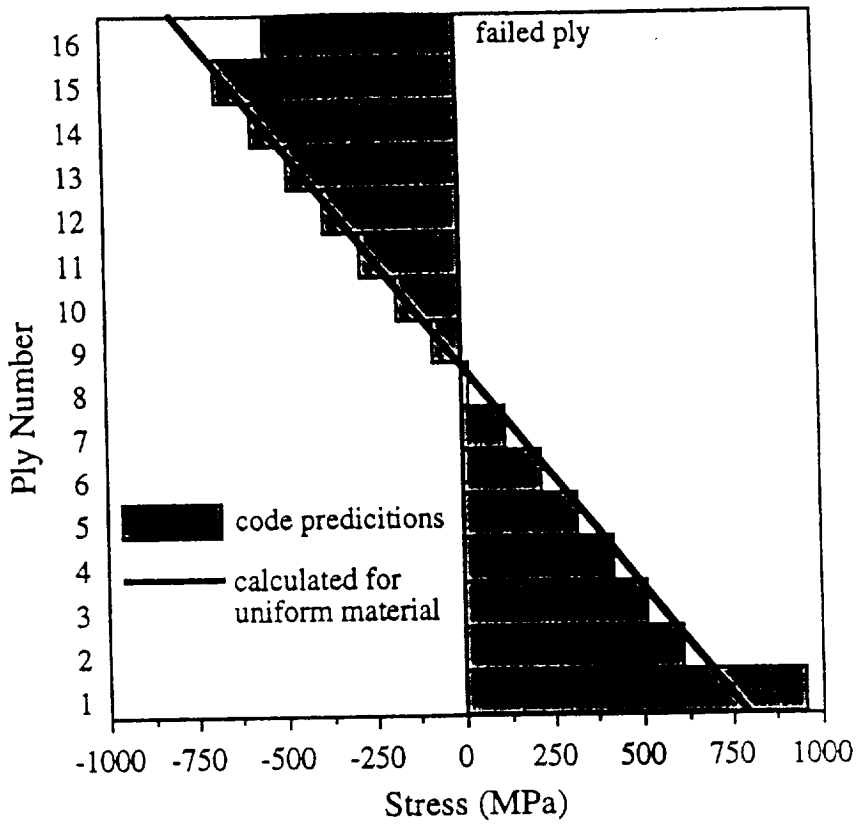

Figure 11. Comparison of ply stresses predicted by code to those calculated assuming uniform material at time of failure for specimens aged 150 hours.